Journal of Cell Science 111, 573-583 (1998)
Printed in Great Britain © The Company of Biologists Limited 1998
JCS4443

Mechanical compression alters proteoglycan deposition and matrix deformation around individual cells in cartilage explants

Thomas M. Quinn[1,2], Alan J. Grodzinsky[1,*], Michael D. Buschmann[2,3], Young-Jo Kim[1] and Ernst B. Hunziker[2]

[1]Continuum Electromechanics Group, Center for Biomedical Engineering, Department of Electrical Engineering and Computer Science, Massachusetts Institute of Technology, Cambridge, MA 02139, USA
[2]M. E. Mueller Institute for Biomechanics, University of Bern, Switzerland
[3]Biomedical Engineering Institute, Ecole Polytechnique, Montreal, Canada
*Author for correspondence

Accepted 14 December 1997: published on WWW 9 February 1998

SUMMARY

We have used new techniques of cell-length scale quantitative autoradiography to assess matrix synthesis, deposition, and deformation around individual chondrocytes in mechanically compressed cartilage explants. Our objectives were to: (1) quantify the effects of static and dynamic compression on the deposition of newly synthesized proteoglycans into cell-associated and further-removed matrices; (2) measure cell-length scale matrix strains and morphological changes of the cell and matrix associated with tissue compression; and (3) relate microscopic physical stimuli to changes in proteoglycan synthesis as functions of compression level and position within mechanically compressed explants. Results indicate a high degree of structural organization in the extracellular matrix, with the pericellular matrix associated with the most rapid rates of proteoglycan deposition, and greatest sensitivity to mechanical compression. Static compression could stimulate directional deposition of secreted proteoglycans around chondrocytes, superimposed on an inhibition of proteoglycan synthesis; these events followed trends for compressive strain in the cell-associated matrix. Conversely, proteoglycan synthesis and pericellular deposition was stimulated by dynamic compression. Results suggest that cell-matrix interactions in the cell-associated matrix may be a particularly important aspect of the chondrocyte response to mechanical compression, possibly involving macromolecular transport limitations and morphological changes associated with fluid flow and local compaction of the matrix around cells.

Key words: Chondrocyte, Proteoglycan, Compression, Autoradiography

INTRODUCTION

Chondrocytes maintain the integrity of the extracellular matrix (ECM) of articular cartilage by mediating the synthesis, secretion, and degradation of matrix proteoglycans (PGs), glycoproteins, and collagens (Heinegard and Oldberg, 1989). These macromolecules assemble in the extracellular space to form an electromechanically and biochemically functional ECM (Grodzinsky, 1983) which is essential to the function of cartilage as a load-bearing, wear-resistant tissue.

Normal joint loading is required for maintenance of articular cartilage structure and function in vivo (Caterson and Lowther, 1978; Jurvelin et al., 1989). Tissue disk and gel/cell culture systems (Schneiderman et al., 1986; Sah et al., 1989; Parkkinen et al., 1992; Burton-Wurster et al., 1993; Buschmann et al., 1995; Lee and Bader, 1995) have enabled characterization of the amplitude and spatial distribution of physical forces and flows within compressed specimens, and the simultaneous quantification of specific biological and biochemical parameters associated with the cellular response (Kim et al., 1994, 1995). Chondrocyte response to static mechanical compression may be associated with direct cell deformation (Guilak et al., 1995; Buschmann et al., 1996a), and could involve structural changes in the cytoskeleton (Ingber, 1993), plasma membrane receptors (Knudson, 1993; Holmvall et al., 1995), and the cell/matrix interface (Hunziker and Schenk, 1984). The role of the ECM as a mediator of cell metabolism (Knudson, 1993) may in turn be affected by static mechanical loading (Sah et al., 1992; Buschmann et al., 1995). This could be due to direct cell-matrix interactions mediated by cell membrane-associated proteins, or physicochemical (e.g. pH, osmotic pressure) changes (Garcia et al., 1994) and transport limitations of cytostimulatory macromolecules (Maroudas, 1976; Garcia et al., 1996). Dynamic compression of cartilage involves fluid flows (Mow et al., 1984) and associated electrokinetic phenomena (Frank and Grodzinsky, 1987) within the electrically charged, poroelastic ECM, which must also be considered as potential mediators of chondrocyte activity.

Tissue-length scale (~0.1-1 mm) spatial distributions of newly synthesized PGs within compressed explant disks have been revealed by explant sectioning (Kim et al., 1994) and

quantitative autoradiography (Buschmann et al., 1996a). Using histological methods, investigators have begun to study chondrocyte response to compression at sub-tissue-length scales. Changes in cell morphology within statically compressed cartilage explants have been observed by confocal microscopy (Guilak et al., 1995) and stereology (Buschmann et al., 1996a). Methods for the measurement of extracellular matrix deformations in compressed cartilage have also been developed (Guilak et al., 1995; Wong et al., 1996; Schinagl et al., 1997). However, physical and biochemical methods to date have not been designed to resolve differences within the ~1-10 μm length scale of the cell-associated (pericellular) and further-removed matrices (Schenk et al., 1986; Mok et al., 1994). Therefore, the roles of these distinct extracellular matrix zones in mediating the chondrocyte response to mechanical compression remain to be elucidated.

We hypothesized that chondrocyte-mediated matrix synthesis and deposition may be particularly sensitive to local biophysical stimuli in the pericellular matrix during tissue compression. Therefore, the aims of this study were to: (1) quantify the effects of static and dynamic compression on the deposition of newly synthesized proteoglycans into cell-associated and further-removed matrices; (2) measure cell-length scale matrix strains and morphological changes of the cell and matrix associated with tissue compression; and (3) relate microscopic physical stimuli to changes in proteoglycan synthesis as functions of compression level and position within mechanically compressed explants. We developed and used novel methods for 1 μm-length scale quantitative autoradiography which allowed for the measurement of matrix deformation and deposition around individual cells in cartilage.

MATERIALS AND METHODS

Tissue culture and mechanical compression

Groups of six 3 mm diameter × 1 mm thick cartilage disks were obtained from the femoropatellar grooves of freshly slaughtered calves and maintained in culture as previously described (Sah et al., 1989). Selected groups of disks were subjected to previously used protocols for static or dynamic compression with impermeable compression platens and without radial confinement (Sah et al., 1989).

Proteoglycan synthesis and deposition

Statically compressed disks were held at 100%, 75%, or 50% of cut thickness (1 mm) for 12 hours and radiolabelled during compression with 10 μCi/ml Na_2-^{35}S-sulfate, and compared with labelled free-swelling controls. Dynamic loading involved 4% amplitude sinusoidal compression at 0 Hz (control), 0.01 Hz, or 0.1 Hz superimposed on static offset compression to 1.0 mm (Sah et al., 1989). Dynamically compressed disks were radiolabelled with 10 μCi/ml Na_2-^{35}S-sulfate for the last 8 hours of a 24 hour compression period. Unincorporated label was removed by washing explants 4 times over 90 minutes in DMEM (Sah et al., 1989) prior to chemical fixation.

Matrix compression

Separate groups were radiolabelled in the free-swelling state for 6 hours with 40 μCi/ml Na_2-^{35}S-sulfate, chased in culture for 3 or 13 days, and then statically compressed to 1 mm or 0.5 mm two hours prior to (and during) chemical fixation, with controls fixed in the free-swelling state. The radiolabel in these latter groups was incorporated into the extracellular matrix well prior to mechanical loading. Therefore, the changes in radiolabel density (by autoradiography) between compression levels were interpreted as an indication of local *matrix volumetric compressive strain* (described below).

Chemical fixation and histological preparation

Samples were chemically fixed with 2% glutaraldehyde (PolySciences Inc.) and 25 mg/ml cetylpyridinium chloride (Sigma) (Hunziker et al., 1992). In statically compressed samples, tissue fixation was performed during compression. Dynamically compressed samples were fixed under free-swelling conditions. Fixed disks were axially bisected and disk halves were dehydrated in a graded water/ethanol series (Merck) and equilibrated in propylene oxide (PPO; Merck). PPO was then exchanged with Epon (48.4% Epon 812 + 35.0% Epon Hardener MNA + 16.6% Epon Hardener DDSA; Fluka) via a graded series, and the explants were embedded in Epon. Semi-thin (1 μm) sections obtained with an ultramicrotome and diamond knife were exposed to an autoradiographic emulsion (Kodak NTB-2) for ~1 week. Following development of the emulsion, samples were stained with 0.008% Toluidine Blue O (Merck). These fixation and embedding methods have previously been shown to reasonably preserve cartilage tissue deformations under static compression (Buschmann et al., 1996a).

Quantitative autoradiography

Semi-automated image analysis techniques were developed for the characterization of cell morphology and cell-associated autoradiography grain distributions as functions of location within explant disks. All measurements were performed on 1 μm thick, explant-bisecting vertical sections (Fig. 1A) oriented on a light microscope stage instrumented with linear displacement encoders (Sony Magnescale) for the determination of locations in tissue sections with an accuracy of ~10 μm. One section was analyzed per explant disk. Digitized high power light microscope (Olympus Vanox) images, 100 μm × 75 μm in total area, with a resolution of 6 pixels/μm, were captured using a CCD color video camera (Sony), frame grabber (RasterOps XLTV) and Macintosh microcomputer. As described in detail below, for each cell section profile sampled, a spatial grid was introduced which was defined in terms of the cell-matrix interface (analogous to geographical techniques of spatial analysis; Unwin, 1981). Data were then expressed in terms of this grid, which allowed for averages to be calculated within corresponding locations around many sampled cells.

Tissue-length scale coordinate description

Tissue sections were parameterized in terms of a circular cylindrical coordinate system (R,θ,Z; Fig. 1A) which was natural to use for explant disks. With the origin of coordinates taken at the geometrical center of the tissue section, the coordinates of the section 'corners' within each quadrant were used to normalize the coordinates at which sampled cells were located (Fig. 1A,B). Symmetry of explant disks and mechanical loading conditions allowed image data to be 'reflected into the first quadrant', after which all chondrocyte positions had normalized radial and axial coordinates between zero (0) and one (1) (Fig. 1B). This allowed for the preservation of extracellular directions with respect to the explant radial and axial directions, and for the identification of selected cell populations (for example, near the radial edge of explant disks).

Sampling

Images were acquired by systematic random sampling (Gunderson and Jensen, 1987) of ~20 locations within each explant cross-section. Cells at each location were then examined for a normal histological appearance and the presence of a well-defined nucleus-cytoplasm interface. Images for analysis were then centered on whichever suitable cell section profile had a nucleus with geometric center closest to the middle of the sampled location. Cells were therefore selected for analysis with a probability which scaled with the nucleus dimensions. Previous studies have demonstrated that variations in

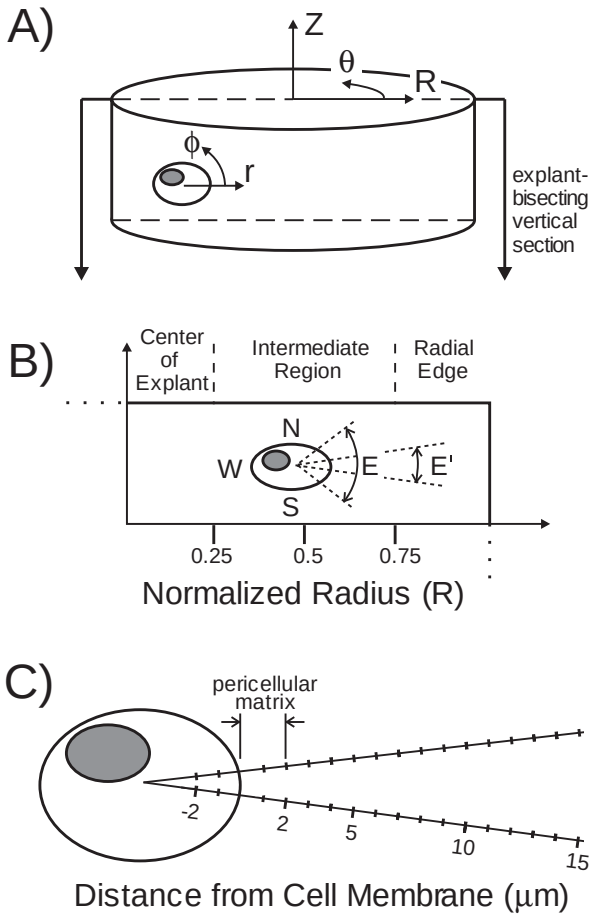

Fig. 1. (A) Data were acquired from explant-bisecting vertical sections of cylindrical cartilage explant disks. Cell-length scale data were expressed by analogy with a polar coordinate (r, ϕ) parameterization around individual cells. Similarly, tissue-length scale locations within explant disks were described in terms of cylindrical polar coordinates (R, θ, Z). (B) Cell images obtained over the entire explant cross-section were reflected such that pericellular directions (N, S, E, W) were related to explant principal axes. Directions were defined such that E represented the $5 \times 2\pi/24$ rad sector oriented toward the nearest explant radial edge, while E′ was similarly oriented but only $2\pi/24$ rad in size. Other directions were defined similarly, with N (and N′) oriented toward the nearest explant axial edge. For data presentation purposes, regions within explant disks were defined as 'center of explant' (between 0 and 25% of disk radius), 'intermediate region' (25-75%), and 'radial edge' (75-100%). (C) Data were also expressed in terms of extracellular distance from the cell membrane (d), which was defined within each $2\pi/24$ rad sector. ECM zones between 0 and 2 μm from the cell membrane were referred to as the pericellular matrix.

nucleus geometry among chondrocytes in calf cartilage are small compared with the mean nucleus geometry (Buschmann et al., 1996a); therefore, our sampling methods were not expected to have introduced any significant bias.

Cell-length scale coordinate description

Colour images were fed to an image processing program (IPLab Spectrum, Signal Analytics Corp.) where a human user traced the cell-matrix boundary of the centrally located cell and autoradiography grains were identified by blue intensity thresholding. The physical space represented within each image was then parameterized in terms of position relative to the traced cell membrane (Fig. 1). The 'coordinate system' employed for this purpose was defined for each image by:

(1) placing a polar coordinate system (r, ϕ, Fig. 1A) at the center of the cell-section profile (at the mean location of the pixels identified by the cell-matrix boundary trace);

(2) discretizing space in the ϕ-direction at $2\pi/24$ rad intervals (Fig. 1B);

(3) identifying the mean r-value of the cell membrane trace within each sector, which provided the profile intercept length (PIL = cell 'radius') as a function of ϕ, and therefore a detailed characterization of cell section profile (cell 'shape');

(4) re-parameterizing the radial coordinate within each sector from its usual meaning in polar coordinates (r) to a new representation (d) given by d = r–PIL(ϕ) representing extracellular distance from the cell membrane; and

(5) discretizing space in the d-direction at 1 μm intervals within each sector (Fig. 1C).

This space parameterization was readily applied to chondrocytes, which previous studies have shown are approximately ellipsoidal (Fig. 2) over a range of compression (Guilak et al., 1995) and almost always possess a single PIL in any direction.

Grain density

Previously developed methods of calculating autoradiography grain density (Buschmann et al., 1996b) were employed within the spatial parameterizations introduced, providing cell-length scale (~1 μm resolution) grain density distributions within the plane of the explant-bisecting vertical sections. Local bulk grain density was also assessed for comparison with previous studies (Kim et al., 1994; Buschmann et al., 1996a), where grain density was averaged over each 100 μm × 75 μm captured image. Independent control studies verified that no significant bias for the calculation of local bulk grain density was introduced through the use of cell-centered images. Background grain density was similarly measured for each tissue section and found to be negligible.

Cell morphometry and stereology

Cell volume fraction (V_V) was estimated by point-counting (Gunderson and Jensen, 1987) of independently sampled images. The PIL(ϕ) data acquired during grain density measurements were also used for automated cell morphometry, either for the estimation of cell volume with the nucleator sizing principle and sine-weighting for isotropic sampling within vertical sections (Gunderson, 1988), or for the description of cell 'shape' (cell 'radius' as a function of direction). Changes in cell volume and PILs between compression levels were interpreted as indications of *cell volumetric compressive strain* and *cell directional compressive strain*, respectively. It is important to note that cell 'shape', as defined within the present study, corresponded to a measurement of cell section profile within individual explant-bisecting vertical sections. This resulted in a lack of morphological information in the explant θ-direction (where mechanical hoop strains may have been significant, for example) as compared to the R, Z-directions (Fig. 1A).

Statistical analyses

Cell PIL, estimated cell volume, and cell- and tissue-length scale grain density data were directly obtained from histological sections, for all applied compression conditions. Positions from which data were acquired were uniformly distributed over explant disks (R, Z; Fig. 1A). Significance tests between data group means acquired at different compression levels but at the same explant positions were performed using the two-tailed Student's *t*-test for distributions with unequal variances. To test for significance of monotonic variations in grain density and morphological indices as a function of radial position (R) within explants at a single compression condition, least squares line and correlation coefficients were obtained, and the significance of the correlation was evaluated by standard methods (Press et al., 1988).

Physical quantities (e.g. matrix and cell strains, changes in PG deposition rates with compression or with pericellular direction) which were subsequently derived from directly obtained data were determined by a two-step procedure: (1) data within two conditions to be considered were expressed as functions of normalized radial position R within ten evenly spaced intervals; and (2) within each interval, data were normalized to the mean of one data set, leaving one data set normalized to the other ('signal' as a function of radial position) and one normalized to itself ('noise'; ten data points, each with a mean of one). Significance tests were then performed between 'signal' and 'noise' data sets for the identification of differences between the two conditions. Differences between data group means acquired at the same explant positions were identified using the above *t*-test. Monotonic variations as a function of radial position (R) were identified by the above *t*-test performed between least squares line slope coefficients (and associated errors), under the assumption of normally distributed measurement errors (Press et al., 1988). Values of $P \geq 0.05$ were considered to be not significant. No investigation of trends as a function of axial position (Z) within explants was performed.

RESULTS

Area density of autoradiography grains on histological sections was directly proportional to volume density of radiolabelled PGs deposited in explants (Buschmann et al., 1996b). Therefore, for samples which had been labelled during mechanical loading, regions of the ECM with elevated grain densities were identified as having more rapidly incorporated newly-synthesized PGs while the loading had been applied (Fig. 2). For samples which had been radiolabelled and chased prior to mechanical compression, elevated grain densities in compressed samples indicated regions of increased compressive strain (i.e. local decreases in matrix volume due to loss of water; Fig. 3).

Using typical values for cell volume and volume fraction, it was possible to estimate characteristic dimensions of the ECM associated with individual cells, based on a concentric spherical geometry (Quinn, 1996); this cell 'domain' was estimated to extend out to d≈8-9 μm from the cell membrane of chondrocytes in FSW explants, and d≈5 μm in 0.5 mm compressed explants. These estimates provided guidelines for the interpretation of cell-length scale autoradiography grain distributions. Within a cell domain, the grain density was assumed to be regulated primarily by the identified cell. At distances from the cell membrane which were near to or greater than these characteristic dimensions, the influences of other nearby cells were expected to become increasingly important, and measured grain densities were interpreted as local averages taken over the domains of several cells.

Proteoglycan synthesis and deposition around individual chondrocytes is affected by the level of static compression and position within explant disks

Autoradiography grain density around individual cells (Fig. 4) revealed markedly anisotropic patterns of PG synthesis and deposition which varied both as a function of the distance (d) from the cell membrane, and as a function of angular position

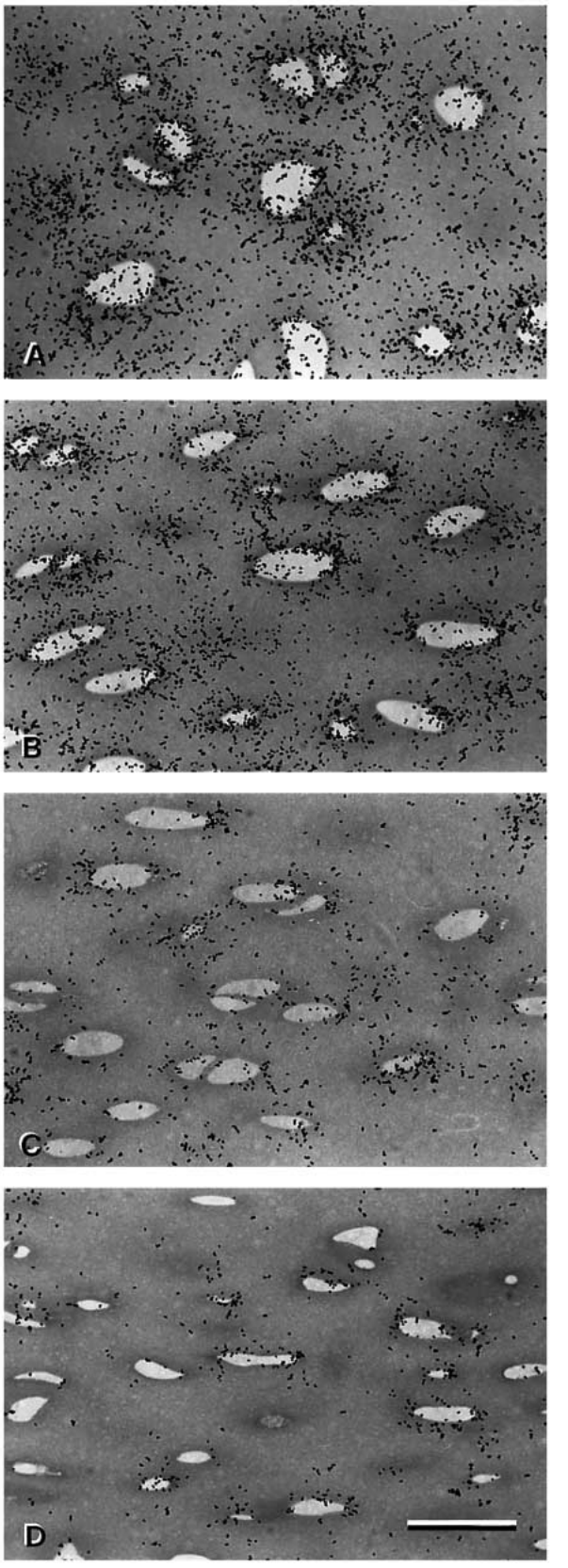

Fig. 2. Autoradiographic histological appearance of chondrocytes and cartilage ECM near the radial edge of calf cartilage disk explants, stained with Toluidine Blue. ^{35}S-sulfate-associated autoradiography grains reveal patterns of PG synthesis and deposition (A) under free-swelling (FSW) conditions, or during tissue compression to (B) 1 mm thickness, (C) 0.75 mm thickness, or (D) 0.5 mm thickness. Bar, 20 μm.

(ϕ) around cells in compressed explants (Fig. 2). In *free-swelling* samples, grain density was highest next to the cell membrane and decreased to a minimum at a distance d ~10 μm from the cell membrane (Fig. 4A,B,C). This spatial pattern of PG deposition did not vary significantly with direction (ϕ) around cells, nor with radial position (R) in free-swelling explants. With increasing static compression to 1 mm (Fig. 4D,E,F), 0.75 mm (Fig. 4G,H,I), and 0.5 mm (Fig. 4J,K,L), grain density around individual chondrocytes remained highest next to the cell membrane (for all ϕ), but decreased overall, most obviously in the central and intermediate regions of explants. Relative to free-swelling controls, all compression levels introduced significant radial (R) gradients in pericellular and local bulk PG deposition rates ($P<0.04$), such that the inhibitory effects of static compression were greatest at the center of explants and least near the radial edge. However, no significant changes in these radial dependences were observed between the 1 mm, 0.75 mm, and 0.5 mm compression levels.

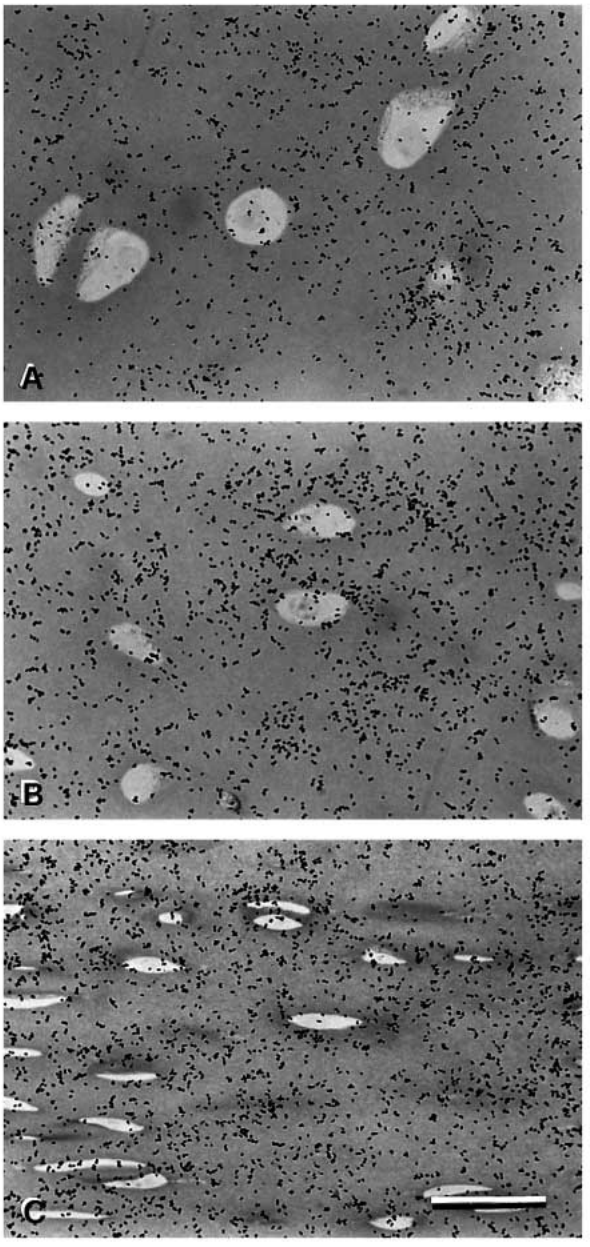

Fig. 3. Autoradiographic histological appearance of chondrocytes and cartilage ECM near the radial edge of calf cartilage disk explants, stained with Toluidine Blue. ^{35}S-sulfate-associated autoradiography grains reveal patterns of PGs deposited 13 days before, and the local deformation (volumetric compressive strain) which occurred when explants were compressed from (A) free-swelling (FSW) conditions to (B) 1 mm thickness and (C) 0.5 mm thickness. Bar, 20 μm.

Directionally dependent PG deposition was also evident around individual cells throughout compressed explant disks. These trends were highlighted by grain density measurement within the narrowest sectors ($2\pi/24$ rad) utilized in the present study. At the unconfined radial edge of compressed explants, PG deposition into the pericellular and further-removed matrices was significantly elevated in the E′ (and W′; data not shown) direction as compared to the S′ (and N′; data not shown) direction (Fig. 4F,I,L; see also Fig. 1B). This directional anisotropy appeared to extend further toward the center of explant disks as compression increased, so that significant directional differences were observed at the center of 0.75 mm disks but not in 1 mm compressed disks (Fig. 4D,G). In 0.5 mm compressed disks, the inhibition of PG synthesis appeared to be so strong that trends for directional anisotropy began to disappear into the noise of the measurement (Fig. 4J,K,L). Interestingly, E′ and W′ directions typically exhibited concomitantly elevated PG deposition rates in the cell-associated matrix. (Statistically significant E′ vs W′ differences in grain density were only observed between 2 μm and 5 μm from the cell membrane, at the radial edge of explants; E′>W′, $P<0.05$). Directional anisotropy was not observed between 11 μm and 15 μm from the cell membrane at any level of compression (Fig. 4). Grain density at this distance from the cell membrane was a reflection of an 'average' behavior taken over the domains of several cells, and no longer associated mainly with a single cell.

Volumetric compression of proteoglycan matrix varies with applied static compression and with position within explant disks

Tissue-length scale

In explants from matrix deformation studies, bulk grain density at each radial (R) position increased monotonically with increasing axial compression (Fig. 5), indicating increases in matrix volumetric compressive strain. This trend was evident at all radial positions within explant disks. Furthermore, compression to 1 mm explant thickness from FSW conditions resulted in greater increases in grain density near the center of explants than near the radial edge ($P<0.02$; Fig. 5), indicating that bulk matrix strain was least near the unconfined radial edge of explant disks.

Cell-length scale

With increasing applied static compression, cell-length scale matrix compressive strain increased monotonically at all R positions within explant disks, within all pericellular ($0<d<2$ μm; Fig. 6) and further-removed matrix zones (data not shown). Significant increases in pericellular matrix compressive strain, averaged over all ϕ-directions, were

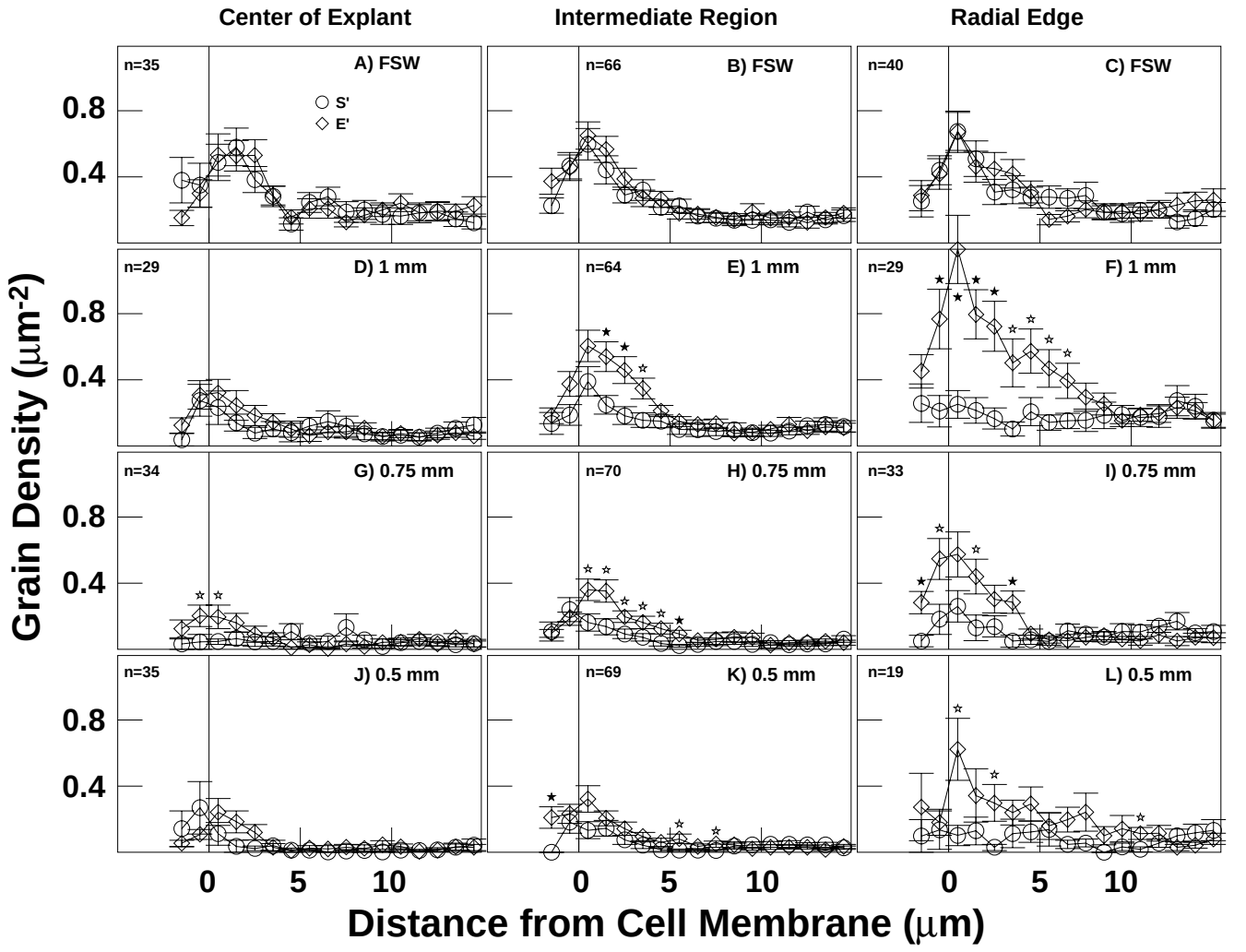

Fig. 4. Effects of static compression on cell-length scale PG synthesis and deposition. Grain density is expressed as a function of distance from the cell membrane d in the S′ (○) and E′ (◇) directions (mean ± s.e.m., *n* = number of cells sampled). Levels of applied compression included free-swelling (A,B,C), 1 mm (D,E,F), 0.75 mm (G,H,I), and 0.5 mm (J,K,L). Cell populations were sampled as a function of radial position R within explants, and include those derived from central (A,D,G,J), intermediate (B,E,H,K), and radial edge (C,F,I,L) regions. ☆ E′≠S′, $P<0.05$; ★ E′≠S′, $P<0.01$ (two-tailed Student's *t*-test; all observed differences were E′>S′).

observed between all successive levels of applied compression ($P<0.001$; not shown). The amount of pericellular PG matrix strain appeared to be consistently less dramatic at the radial edge of explant disks (Fig. 6C,F,I,L) as compared to central (Fig. 6A,D,G,J) and intermediate (Fig. 6B,E,H,K) regions. This R-dependence of pericellular matrix compressive strain was particularly significant in samples compressed to 0.5 mm (W′ and N′; $P<0.002$). In addition, at the radial edge of explants compressed to 1 mm, pericellular matrix compression appeared to be directional, with N′ and S′ directions being more compressed than E′ and W′ directions (this trend was clear (Fig. 6C,F,I,L) but not significant as defined within the present study). Similar trends were observed within cell-associated matrix zones between 2 and 5 μm from the cell membrane (Quinn, 1996). As expected, effects of compression on PG matrix strain within matrix zones greater than ~5 μm from the cell membrane were consistent with tissue-length scale trends (Fig. 5).

Some cell morphological indices within explant-bisecting vertical sections vary significantly with compression and with position within explant disks

Consistent with previous results (Buschmann et al., 1996a), estimated cell volume in all compressed samples decreased significantly ($P<0.001$) relative to free-swelling controls (Fig. 7). Cell volume fraction (V_V) was not found to vary systematically with increasing amplitude of static compression, at any location within explants (Quinn, 1996). Combining V_V with corresponding cell volume data (Fig. 7) revealed a trend toward increasing cell number density (N_V) with increasing compression ($P<0.03$). However, no significant radial (R) dependences were observed in cell volume, V_V, or N_V at any level of applied compression, or in cell volumetric strain (between compression levels) (Quinn, 1996).

In general, increasing static compression was associated with decreased cell radii in the direction of compression ('vertical'), while cell horizontal radii were unchanged. PILs (cell 'radii') in N′ and S′ directions decreased between all

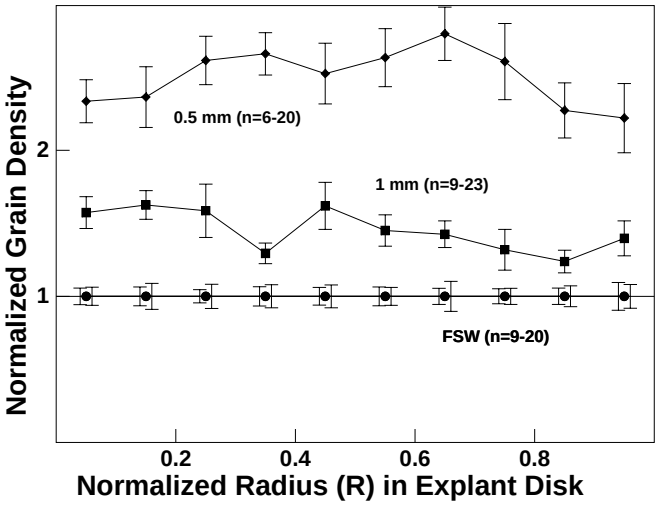

Fig. 5. Tissue-length scale autoradiography grain density for cartilage explants radiolabelled several days prior to being subjected to graded levels of static compression. Local bulk grain density data (mean ± s.e.m., *n* = number of tissue images sampled) from free-swelling (FSW; ●) samples, and from samples compressed to 1 mm (■) and 0.5 mm (◆) were normalized to the mean of free-swelling values at each normalized radial position in explant disks. Dual error bars on FSW data reflect the fact that compressed samples (1 mm and 0.5 mm) had different controls in this measurement. Error bars to left are for 1 mm controls; error bars to right are for 0.5 mm controls.

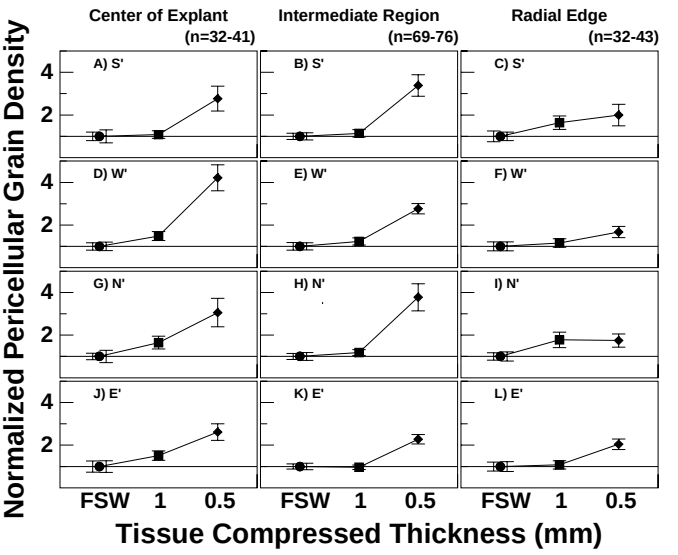

Fig. 6. Effects of static compression on pericellular PG matrix compressive strain. For 0 μm < d < 2 μm (Fig. 1C), grain densities under FSW conditions (●) and in samples compressed to 1 mm (■) and 0.5 mm (◆) have been normalized to the mean of the FSW value, and plotted for comparison as a function of radial position within explants, and include those derived from central (A,D,G,J), intermediate (B,E,H,K), and radial edge (C,F,I,L) regions. Directions considered included S′ (A,B,C), W′ (D,E,F), N′ (G,H,I), and E′ (J,K,L). Dual error bars on FSW data reflect the fact that compressed samples (1 mm and 0.5 mm) had different controls in this measurement. Error bars to left are for 1 mm controls; error bars to right are for 0.5 mm controls (mean ± s.e.m., *n* = number of cells sampled).

successive compression levels (P<0.04) (Fig. 7), similar to trends previously observed in cells near the center of compressed explant disks (Buschmann et al., 1996a). PILs in the E′ and W′ directions did not change significantlyrelative to free-swelling controls, at any level of applied compression. Within explant disks at a single compression level, radial (R) dependences in cell PILs were observed in some ϕ-directions within explants under FSW conditions (Fig. 7A,B,C), and under compression to 1 mm (Fig. 7D,E,F) and 0.75 mm (Fig. 7G,H,I). Relative to free-swelling controls, samples compressed to 0.75 mm also exhibited R-dependent cell directional compressive strain in ϕ-directions near NE and SW (Fig. 7G,H,I), such that the effects of static compression were greatest near the center of explants.

Dynamic compression: cell-length scale patterns of PG matrix deposition depend on compression frequency and position within explant disks

At the 1.0 mm offset thickness used in dynamic compression experiments, directional anisotropy of PG matrix synthesis around individual chondrocytes was consistent with what had been observed under static compression (Fig. 4). Even though dynamically compressed samples were chemically fixed under free-swelling conditions, anisotropy existed emphasizing, for example, the E direction over the S direction (Quinn, 1996). This directional bias was relatively small, and did not appear to be markedly influenced by the frequency of dynamic compression. Therefore, grain density data were averaged over all measured extracellular directions (ϕ = 0 to 2π rad) for comparison between compression frequencies.

Relative to 0 Hz controls, effects of dynamic compression at 0.01 and 0.1 Hz on PG synthesis were always stimulatory. At the radial edge of explants, with increasing compression frequency, PG deposition rates were consistently and significantly elevated around chondrocytes in all matrix zones (Fig. 8C,F,I). Similar trends were also observed in the intermediate regions (Fig. 8B,E,H). At the center of explants, dynamic compression also had a stimulatory effect which was more significant at 0.01 Hz than at 0.1 Hz in the pericellular matrix (Fig. 8A,D,G). Relative to 0 Hz controls, stimulation of PG deposition did not depend on radial position (R) within explants for 0.01 Hz dynamic compression, but was significantly R-dependent at 0.1 Hz, both in the pericellular matrix (P<0.001) and when measured as a local bulk quantity (P<0.02).

DISCUSSION

Proteoglycan synthesis and deposition into the pericellular and further-removed matrices around chondrocytes varied with the level of applied compression and with position (R) within radially unconfined cartilage explant disks. The pericellular matrix was associated with the most rapid rates of proteoglycan deposition, and greatest sensitivity to static and dynamic mechanical compression. Several microphysical stimuli were also identified which exhibited similar compression-dependent trends, and which therefore may be important mediators of the chondrocyte response to mechanical compression. In particular, our results suggest that local matrix volumetric

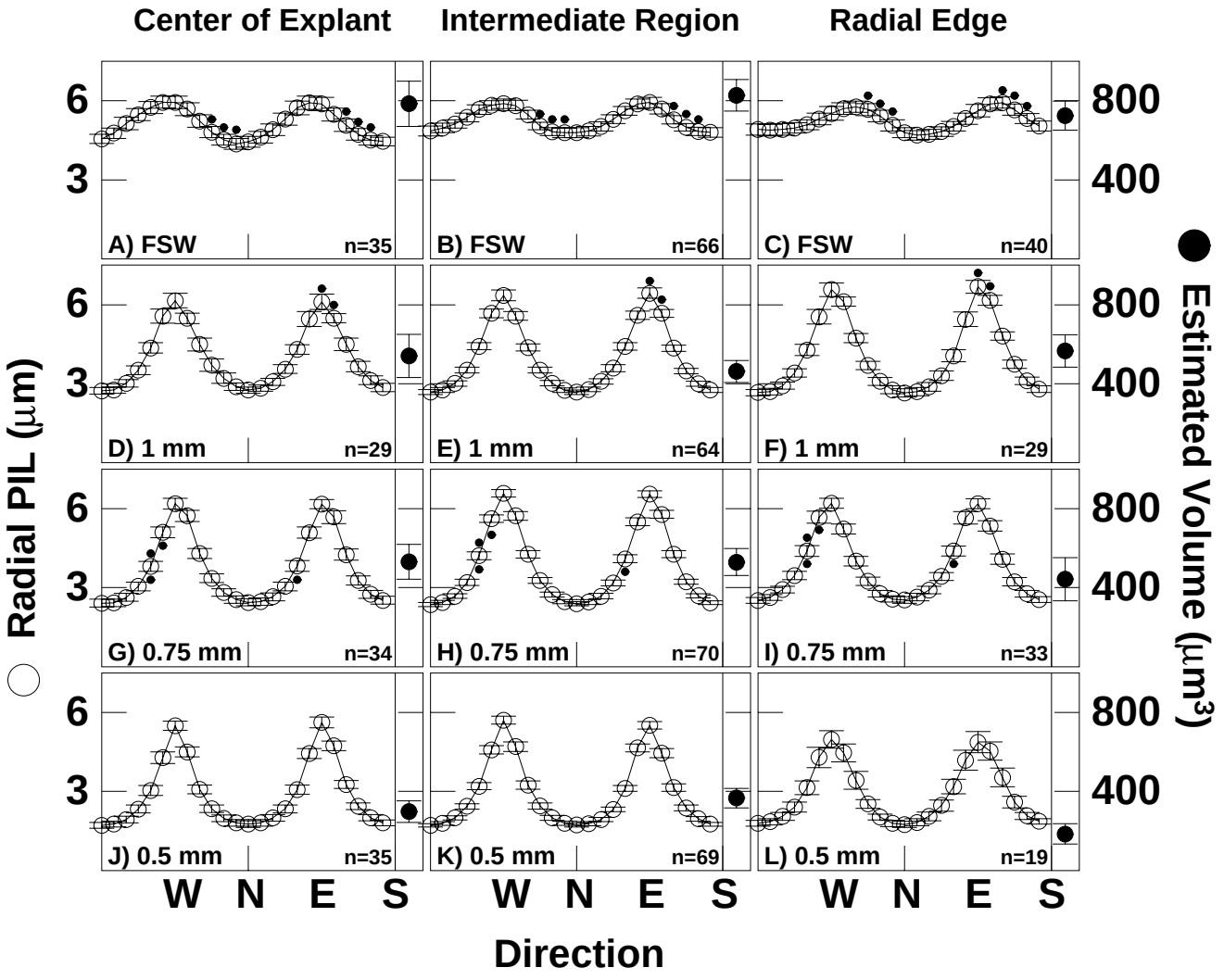

Fig. 7. Effects of static compression on cell shape and estimated cell volume. Radial profile intercept length (PIL; cell 'radius' on cross-section) is expressed as a function of ϕ-direction. Levels of applied compression included free-swelling (A,B,C), 1 mm (D,E,F), 0.75 mm (G,H,I), and 0.5 mm (J,K,L). Cells were sampled as a function of radial position R within explants, and include those derived from central (A,D,G,J), intermediate (B,E,H,K), and radial edge (C,F,I,L) regions. Dots above or below data points indicate ϕ-directions where significant (P<0.05) R-dependent trends were observed for PIL or cell directional strain, respectively (mean ± s.e.m., n = number of cells sampled).

strain, fluid flows, and cell-matrix interactions in the pericellular matrix may be especially important stimuli to chondrocytes.

PG deposition rates are highest in the cell-associated (pericellular) matrix and are sensitive to mechanical compression

The rate of PG deposition varied significantly with distance from the cell membrane, and was consistently highest in the cell-associated (pericellular) matrix. This trend was evident in free-swelling explants (Fig. 4A,B,C), and persisted during static and dynamic compression (Figs 4D-L and 8). These observations are consistent with previous studies which highlighted the cell-associated matrix as a distinct extracellular matrix zone (Schenk et al., 1986) possessing a unique metabolic PG pool (Mok et al., 1994). Furthermore, effects of tissue mechanical compression on PG matrix compression and deposition were most dramatic in the cell-associated matrix, suggesting that this zone may play a particularly important role in the chondrocyte response to mechanical compression.

Proteoglycan matrix deposition around individual chondrocytes becomes directionally-dependent under static compression

Under free-swelling conditions, PG matrix deposition rates did not vary significantly with direction (ϕ) around chondrocytes. This suggests that cells in free-swelling calf cartilage explants perceive and maintain their extracellular environment without directional bias. During tissue static compression, however, PG deposition around chondrocytes became directionally dependent, with the most rapid rates of deposition occurring in directions perpendicular to that of applied compression. This suggests that some aspects of the microphysical environments of chondrocytes in uniaxially compressed, radially unconfined explants were directional in character, and that these factors

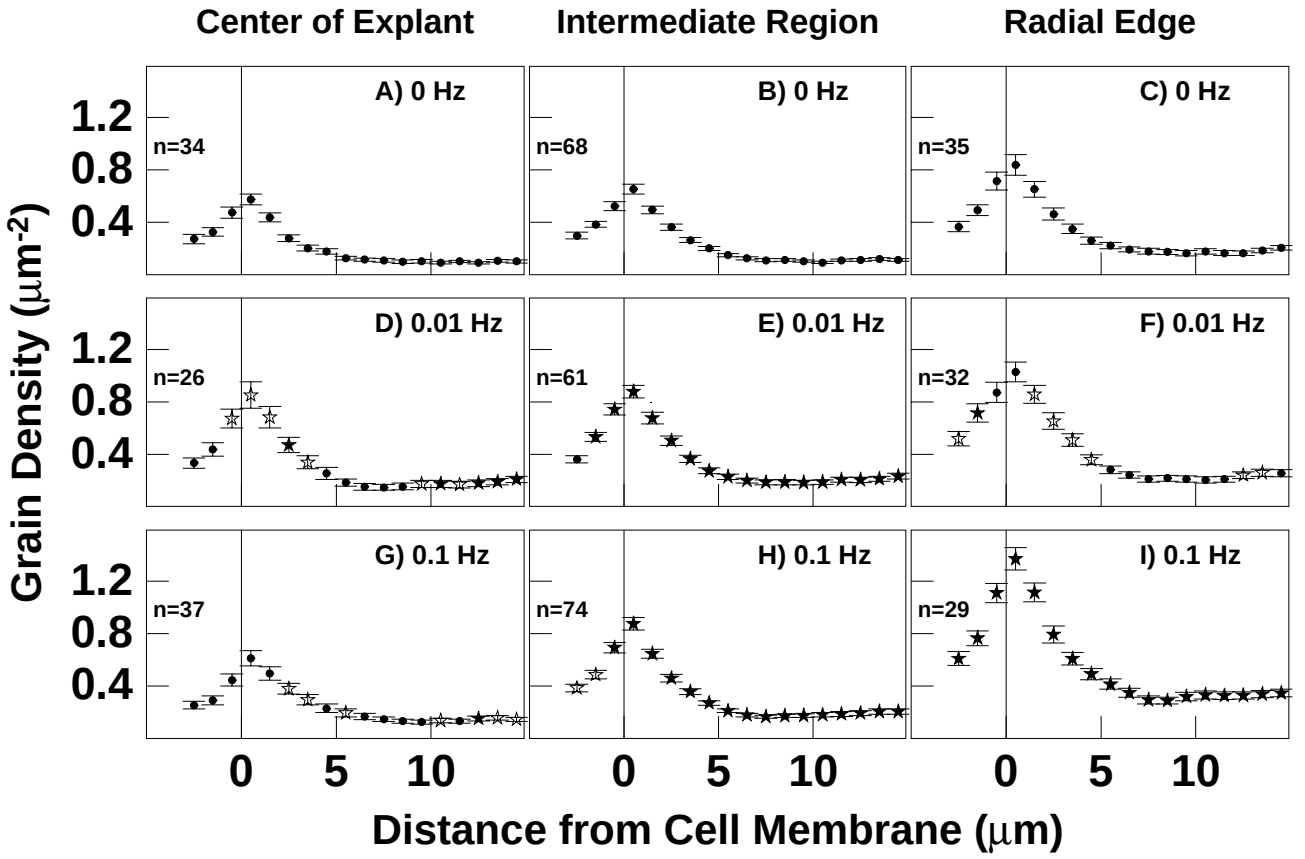

Fig. 8. Effects of dynamic compression on cell-length scale PG synthesis and deposition. Grain density is expressed as a function of distance from the cell membrane d averaged over all ϕ-directions (mean ± s.e.m., *n* = number of cells sampled). Frequencies of applied compression included 0 Hz (A,B,C), 0.01 Hz (D,E,F), and 0.1 Hz (G,H,I). Cells were sampled as a function of radial position R within explants, and include those derived from central (A,D,G), intermediate (B,E, H), and radial edge (C,F,I) regions. Values different from those for 0 Hz (by two-tailed Student's *t*-test; all observed differences were increases) are indicated by ☆ ($P<0.05$) or ★ ($P<0.01$).

were important regulators of PG matrix assembly at the cell-length scale.

Bulk and pericellular matrix compression varied consistently with PG synthesis across level of static compression and position within explants

Local bulk matrix compressive strain increased monotonically with static compression at all observed locations within explant disks (Fig. 5). In explants compressed to 1 mm thickness from FSW conditions, these increases were significantly larger near the center of explants than near the radial edge. Concomitantly, local bulk PG synthesis rates were observed to decrease with tissue static compression, but were less affected at larger radial positions R within explant disks. PG synthesis therefore appeared to vary inversely with measured matrix compressive strain, both as a function of applied static compression thickness, and as a function of radius within compressed explant disks. These associations suggest that local matrix compressive strain represents a physical stimulus to chondrocytes in statically compressed cartilage explants which consistently correlates with decreases in PG synthesis (as a function of applied compression and as a function of position within explants at a given compression).

At the cell-length scale, matrix compressive strain was consistently increased with tissue static compression in all extracellular matrix zones. In addition, the increase in matrix strain in the pericellular zone was less dramatic at the radial edge of explant disks compressed to 0.5 mm than in the central regions (Fig. 6), indicating that tissue static compression had less of an effect on pericellular matrix compressive strain at increasing radii within explant disks. Furthermore, compression-induced increases in pericellular matrix compressive strain appeared to be directionally dependent at the radial edge of explants compressed to 1 mm, where pericellular PG deposition was also most strongly directional; regions above and below cells (with the vertical defined by the compression axis) exhibited the highest matrix strains and the lowest PG deposition rates. Due to its close proximity to the cell, the pericellular matrix may be expected to have the most direct influence on cellular metabolism, as compared with other ECM zones. Therefore, these results further suggest that cell-associated (pericellular) matrix compressive strain may be a particularly important part of the process by which matrix compressive strain mediates the chondrocyte response to compression.

PG synthesis and deposition rates are associated with changes in cell morphology within explant-bisecting vertical sections

With increasing static compression, trends for changes in cell

volume, cell number density, and cell directional radii were all in agreement with previous observations (Guilak et al., 1995; Buschmann et al., 1996a; Wong et al., 1996). However, neither the estimated volume nor number density of chondrocytes varied significantly with radial position R within compressed explants. In some cases, cell radii in individual ϕ-directions varied systematically with radial position R within explants (Fig. 7); however, these trends were inconsistent with trends for PG synthesis (Fig. 4) in that they were strongest in FSW explants (where PG synthesis was only weakly dependent upon R) and weakest during compression (where PG synthesis was strongly dependent on R). Therefore, the results do not support the hypothesis that these cell morphological indices play important roles in modulating the tissue-length scale radial variations in PG synthesis in compressed cartilage. In contrast, cell directional strains in 0.75 mm compressed samples (relative to FSW samples) were observed to follow trends for PG synthesis as a function of radial position R within explants. These observations included significant trends for cell-directional strains in ϕ-directions *between* the principal axes (in 'NE' and 'SW' directions; Fig. 7G,H,I), suggesting a potential role (and measurement technique) for cell and matrix shear strains as metabolically-relevant cell stimuli within mechanically compressed cartilage. Therefore, morphometry results obtained from explant-bisecting vertical sections indicated that trends for cell directional strains (cell shape *changes*) were consistent with trends for the chondrocyte metabolic response to compression.

Dynamic compression: proteoglycan matrix deposition around individual chondrocytes follows tissue-length scale patterns of fluid flow

At the cell-length scale, stimulation of PG synthesis and deposition during dynamic compression was most dramatic in the cell-associated (pericellular) matrix. At the radial edge of explant disks, this stimulation increased monotonically with increasing frequency of dynamic compression, while at the center of explant disks, stimulation was greater at 0.01 Hz than at 0.1 Hz (Fig. 8). In agreement with these trends are theoretically anticipated oscillatory fluid flow amplitudes; based on a previous study (Kim et al., 1995), these amplitudes were expected to increase monotonically with compression frequency at the radial edge of explants, but be similar at 0.01 Hz and 0.1 Hz near the center of explants under the conditions of the present study. Therefore, stimulation of PG synthesis and deposition rates closely followed anticipated trends for oscillatory fluid flow amplitudes.

Microphysical regulation of proteoglycan synthesis and matrix assembly in compressed cartilage explants: possible mechanisms

The identification of microphysical mediators of metabolism is important to the understanding of the chondrocyte phenotype in both health and disease, and to the optimization of strategies for cartilage maintenance and repair. Potential mechanisms by which tissue deformations may be transduced into metabolic responses by chondrocytes have been discussed extensively in the literature (Sah et al., 1992; Guilak et al., 1995; Buschmann et al., 1996a; Grodzinsky et al., 1997). Results of the present study suggest that cell-matrix interactions in the cell-associated matrix may be a particularly important aspect of this transduction; these cell-matrix interactions may involve macromolecular transport limitations and/or morphological changes associated with local compaction of the matrix around cells (Figs 5, 6).

It is well known that secreted cell products, including newly-synthesized extracellular matrix macromolecules, can influence cell metabolism and matrix synthesis (Lucas and Dziewiatkowski, 1987; Larsson et al., 1989). Furthermore, transport of macromolecules through the cartilage ECM is likely to be a complex process of 'hindered diffusion-reaction', as these large solutes move through the tortuous network of glycosaminoglycans, collagen fibrils, and potential binding sites which form the cartilage ECM (Grodzinsky, 1983). As a consequence, static compression of cartilage may significantly impede these transport processes by causing a decrease in the characteristic pore size through which these macromolecules must penetrate, and an increase in the density of binding sites. Dynamic compression and associated oscillatory fluid flows, on the other hand, may be expected to enhance macromolecular transport rates within the cartilage ECM (Brenner and Edwards, 1993; Garcia et al., 1996), even with the low dynamic strain amplitudes and frequencies used here (Kim et al., 1995). Therefore, newly synthesized and secreted macromolecules would be expected to move relatively slowly through the extracellular space next to chondrocytes in statically compressed cartilage, and to be transported more quickly away from chondrocytes during tissue dynamic compression. If chondrocyte synthesis of ECM macromolecules is affected by the concentrations of recently-secreted macromolecules adjacent to their cell membrane (perhaps through interactions with cell-surface proteins sensitive to post-secretion changes (Sah et al., 1990; Knudson et al., 1997), then extracellular transport limitations of newly synthesized macromolecules could significantly affect chondrocyte metabolic responses to both static and dynamic compression, consistent with experimental trends at tissue- and cell-length scales.

Morphological changes of cells and intracellular organelles may represent additional, potentially concomitant regulatory mechanisms. The present study also highlighted a directional aspect to matrix assembly during static compression. Potential mechanisms for this behavior include cell and organelle morphological changes, cell-matrix interactions, and localized mechanical deformations in the ECM which resulted in directional secretion, extracellular transport, and deposition of matrix macromolecules. Results may also suggest a role for intracellular organizational changes such that the nucleus moves to the 'center' of the cell (Fig. 3) while the Golgi and secretory apparatus move to the cell periphery and secretion is biased to occur in directions perpendicular to that of applied static compression.

This work was supported by NIH Grant AR33236, AO/ASIF Grant 95-W63, and a fellowship from Merck Research Laboratories (TMQ). We thank Sophia T. Kung and David Thacher for helpful discussions, and E. Berger, V. Gaschen, E. Kapfinger, A. Maung, A. Maurer, P. Perumbuli, M. Ponticiello, and C. Waite for technical contributions.

REFERENCES

Brenner, H. and Edwards, D. A. (1993). *Macrotransport Processes.* Butterworth-Heinemann, Stoneham MA.

Burton-Wurster, N., Vernier-Singer, M., Farquhar, T. and Lust, G. (1993). Effect of compressive loading and unloading on synthesis of total protein, proteoglycan, and fibronectin by canine cartilage explants. *J. Orthop. Res.* **11**, 717-729.

Buschmann, M. D., Gluzband, Y. A., Grodzinsky, A. J. and Hunziker, E. B. (1995). Mechanical compression modulates matrix biosynthesis in chondrocyte/agarose culture. *J. Cell Sci.* **108**, 1497-1508.

Buschmann, M. D., Hunziker, E. B., Kim, Y.-J. and Grodzinsky, A. J. (1996a). Altered aggrecan synthesis correlates with cell and nucleus structure in statically compressed cartilage. *J. Cell Sci.* **109**, 499-508.

Buschmann, M. D., Maurer, A. M., Berger, E. and Hunziker, E. B. (1996b). A method of quantitative autoradiography for the spatial localization of proteoglycan synthesis rates in cartilage. *J. Histochem. Cytochem.* **44**, 423-431.

Caterson, B. and Lowther, D. A. (1978). Changes in the metabolism of the proteoglycans from sheep articular cartilage in response to mechanical stress. *Biochim. Biophys. Acta* **540**, 412-422.

Frank, E. H. and Grodzinsky, A. J. (1987). Cartilage electromechanics – I. Electrokinetic transduction and the effects of electrolyte pH and ionic strength. *J. Biomech.* **20**, 615-627.

Garcia, A. M., Black, A. C. and Gray, M. L. (1994). Effects of physicochemical factors on the growth of mandibular condyles in vitro. *Calcif. Tissue Int.* **54**, 499-504.

Garcia, A. M., Frank, E. H., Grimshaw, P. E. and Grodzinsky, A. J. (1996). Contributions of fluid convection and electrical migration to transport in cartilage: Relevance to loading. *Arch. Biochem. Biophys.* **333**, 317-325.

Grodzinsky, A. J. (1983). Electromechanical and physicochemical properties of connective tissue. *CRC Crit. Rev. Biomed. Eng.* **9**, 133-199.

Grodzinsky, A. J., Kim, Y.-J., Buschmann, M. D., Garcia, M. L., Quinn, T. M. and Hunziker, E. B. (1998). Response of the chondrocyte to mechanical stimuli. In *Osteoarthritis* (ed. K. D. Brandt, S. Lohmander and M. Doherty), pp. 123-136. Oxford University Press.

Guilak, F., Ratcliffe, A. and Mow, V. C. (1995). Chondrocyte deformation and local tissue strain in articular cartilage: A confocal microscopy study. *J. Orthop. Res.* **13**, 410-421.

Gunderson, H. J. G. and Jensen, E. B. (1987). The efficiency of systematic sampling in stereology and its prediction. *J. Microsc.* **147**, 229-263.

Gunderson, H. J. G. (1988). The nucleator. *J. Microsc.* **151**, 3-21.

Heinegard, D. and Oldberg, A. (1989). Structure and biology of cartilage and bone matrix noncollagenous macromolecules. *FASEB J.* **3**, 2042-2051.

Holmvall, K., Camper, L., Johansson, S., Kimura, J. H. and Lundgren-Akerlund, E. (1995). Chondrocyte and chondrosarcoma cell integrins with affinity for collagen type II and their response to mechanical stress. *Exp. Cell Res.* **221**, 496-503.

Hunziker, E. B. and Schenk, R. K. (1984). Cartilage ultrastructure after high pressure freezing, freeze substitution and low temperature embedding II. Intercellular matrix ultrastructure – preservation of proteoglycans in their native state. *J. Cell Biol.* **98**, 277-282.

Hunziker, E. B., Ludi, A. and Hermann, W. (1992). Preservation of cartilage matrix proteoglycans using cationic dyes chemically related to ruthenium hexaamine trichloride. *J. Histochem. Cytochem.* **40**, 909-917.

Ingber, D. (1993). Cellular tensegrity: Defining new rules of biological design that govern the cytoskeleton. *J. Cell Sci.* **104**, 613-627.

Jurvelin, J., Kiviranta, I., Saamanen, A.-M., Tammi, M. and Helminen, H. J. (1989). Partial restoration of immobilization-induced softening of canine articular cartilage after remobilization of the knee (stifle) joint. *J. Orthop. Res.* **7**, 352-358.

Kim, Y. J., Sah, R. L. Y., Grodzinsky, A. J., Plaas, A. H. K. and Sandy, J. D. (1994). Mechanical regulation of cartilage biosynthetic behavior: Physical stimuli. *Arch. Biochem. Biophys.* **311**, 1-12.

Kim, Y. J., Bonassar, L. J. and Grodzinsky, A. J. (1995). The role of cartilage streaming potential, fluid flow, and pressure in the stimulation of chondrocyte biosynthesis during dynamic compression. *J. Biomech.* **28**, 1055-1066.

Knudson, C. B. (1993). Hyaluronan receptor-directed assembly of chondrocyte pericellular matrix. *J. Cell Biol.* **120**, 825-834.

Knudson, C. B., Constable, C. T. and Nofal, G. A. (1997). Changes in phosphorylation and actin-association of CD44 with receptor occupancy on articular chondrocytes. In *Transactions of the 43rd Annual Meeting*. p. 34. Orthopaedic Research Society, San Francisco.

Larsson, T., Aspden, R. M. and Heinegard, D. (1989). Large cartilage proteoglycan (PG-LA) influences the biosynthesis of macromolecules by isolated chondrocytes. *Matrix* **9**, 343-352.

Lee, D. A. and Bader, D. L. (1995). The development and characterization of an in vitro system to study strain-induced cell deformation in isolated chondrocytes. *In Vitro Cell Dev. Biol.* **31**, 828-835.

Lucas, P. A. and Dziewiatkowski, D. D. (1987). Feedback control of selected biosynthetic activities of chondrocytes in culture. *Conn. Tiss. Res.* **16**, 323-341.

Maroudas, A. (1976). Transport of solutes through cartilage: Permeability to large molecules. *J. Anat.* **122**, 335-347.

Mok, S. S., Masuda, K., Hauselmann, H. J., Aydelotte, M. B. and Thonar, E. J. M. A. (1994). Aggrecan synthesized by mature bovine chondrocytes suspended in alginate. *J. Biol. Chem.* **269**, 33021-33027.

Mow, V. C., Holmes, M. H. and Lai, W. M. (1984). Fluid transport and mechanical properties of articular cartilage: A review. *J. Biomech.* **17**, 377-394.

Parkkinen, J. J., Lammi, M. J., Helmminen, H. J. and Tammi, M. (1992). Local stimulation of proteoglycan synthesis in articular cartilage explants by dynamic compression in vitro. *J. Orthop. Res.* **10**, 610-620.

Press, W. H., Flannery, B. P., Teukolsky, S. A. and Vetterling, W. T. (1988). *Numerical Recipes in C*. Cambridge University Press, Cambridge, UK.

Quinn, T. M. (1996). Articular cartilage: Matrix assembly, mediation of chondrocyte metabolism and response to compression. PhD thesis, Massachusetts Institute of Techology, Cambridge, MA.

Sah, R. L.-Y., Kim, Y.-J., Doong, J.-Y. H., Grodzinsky, A. J., Plaas, A. H. K. and Sandy, J. D. (1989). Biosynthetic response of cartilage explants to dynamic compression. *J. Orthop. Res.* **7**, 619-636.

Sah, R. L.-Y., Grodzinsky, A. J., Plaas, A. H. K. and Sandy, J. D. (1990). Effects of tissue compression on the hyaluronate-binding properties of newly synthesized proteoglycans in cartilage explants. *Biochem. J.* **267**, 803-808.

Sah, R. L.-Y., Grodzinsky, A. J., Plaas, A. H. K. and Sandy, J. D. (1992). Effects of static and dynamic compression on matrix metabolism in cartilage explants. In *Articular Cartilage Biochemistry and Osteoarthritis* (ed. K. E. Kuettner, V. C. Hascall and R. Schleyerbach), pp. 373-392. Raven Press, New York.

Schenk, R. K., Eggli, P. S. and Hunziker, E. B. (1986). Articular cartilage morphology. In *Articular Cartilage Biochemistry* (ed. K. E. Kuettner, R. Schleyerbach and V. C. Hascall), pp. 3-22. Raven Press, New York.

Schinagl, R. M., Gurskis, D., Chen, A. C. and Sah, R. L. (1997). Depth-dependent confined compression modulus of full-thickness bovine articular cartilage. *J. Orthop. Res.* **15**, 499-506.

Schneiderman, R., Kevet, D. and Maroudas, A. (1986). Effects of mechanical and osmotic pressure on the rate of glycosaminoglycan synthesis in the human adult femoral head cartilage: an in vitro study. *J. Orthop. Res.* **4**, 393-408.

Unwin, D. J. (1981). *Introductory Spatial Analysis*. Methuen, New York.

Wong, M., Wuethrich, P., Eggli, P. and Hunziker, E. (1996). Zone-specific cell biosynthetic activity in mature bovine articular cartilage: A new method using confocal microscopic stereology and quantitative autoradiography. *J. Orthop. Res.* **14**, 424-432.